



Contents lists available at ScienceDirect

Catena

journal homepage: www.elsevier.com/locate/catena

Stratigraphy of near-valley head quaternary deposits and evidence of climate-driven slope-channel processes in southern Brazilian highlands

Marcelo Accioly Teixeira de Oliveira ^{a,*}, Hermann Behling ^b, Luiz Carlos Ruiz Pessenda ^c, Gisele Leite de Lima ^a

^a Departamento de Geociências, CFH, Universidade Federal de Santa Catarina (UFSC), Caixa Postal 5175, cep: 88040-970, Trindade, Florianópolis, Santa Catarina, Brazil

^b Department of Palynology and Climate Dynamics, Albrecht-von-Haller-Institute for Plant Sciences, University of Göttingen, Untere Karspüle 2, D-37073, Göttingen, Germany

^c Centro de Energia Nuclear na Agricultura, Laboratório de C 14, Universidade de São Paulo (USP), Avenida Centenário no. 303, São Dimas, cep: 13416000, Piracicaba, São Paulo, Brazil

ARTICLE INFO

Article history:
Available online xxxxx

Keywords:
Colluvium
Stratigraphy
Quaternary
Climate changes
Environmental changes

ABSTRACT

During the past 40 years colluvial and alluvial deposits have been used in Brazil as good indicators of regional landscape sensitivity to Quaternary environmental changes. In spite of the low resolution of most of the continental sedimentary record, geomorphology and sedimentology may favor palaeoenvironmental interpretation when supported by independent proxy data. This paper presents results obtained from pedostratigraphic sequences, in near-valley head sites of southern Brazilian highlands, based on geomorphologic, sedimentologic, micromorphologic, isotopic and palynologic data. Results point to environmental changes, with ages that coincide with Marine Isotopic Stages (MIS) 5b; 3; 2 and 1. During the late Pleistocene, although under temperatures and precipitation lower than today, the local record points to relatively wet local environments, where shallow soil-water saturated zones contributed to erosion and sedimentation during periods of climatic change, as during the transition between MIS 2 and MIS 1. Late Pleistocene events with ages that coincide with the Northern Hemisphere Younger Dryas are also depicted. During the mid Holocene, slope-wash deposits suggest a climate drier than today, probably under the influence of seasonally contrasted precipitation regimes. The predominance of overland flow-related sedimentary deposits suggests an excess of precipitation over evaporation that influenced local palaeohydrology. This environmental condition seems to be recurrent and explains how slope morphology had influenced pedogenesis and sedimentation in the study area. Due to relative sensitiveness, resilience and short source-to-sink sedimentary pathways, near-valley head sites deserve further attention in Quaternary studies in the humid tropics.

© 2008 Published by Elsevier B.V.

1. Introduction

During the past 40 years the study of erosive and sedimentary processes in topographic hollows has been a common topic for Brazilian research in geomorphology and quaternary geology (Bigarella and Mousinho, 1965; Meis and Machado, 1978; Meis and Moura, 1984; Moura et al., 1991). Since the 1960s, the role of the so-called colluvial ramps as slope-channel coupling landforms is emphasized on the basis of sedimentary evidence (Bigarella and Mousinho, 1965; Meis and Moura, 1984). More recently, the role of topographic hollows connected to the drainage network was approached into the far-reaching theoretical framework of the channel-heads characterization and modeling (Dietrich and Dunne, 1993). Erosive and sedimentary cycles and hemicycles, surges of geomorphic processes and their connection to environmental controlling factors are important issues for geomorphology and Quaternary geology studies because they allow drawing inferences about climatic teleconnections and millennial oscillations that seem realistic in terms of the information

produced by proxy ice-core records (Aharon and Chappell, 1986; Coltrinari, 1993; Iriondo, 1999; Thomas, 2004).

As proposed earlier (Bigarella and Mousinho, 1965; Meis and Monteiro, 1979), alluvial and colluvial deposits are widely recognized today as good indicators of local and regional landscape sensitivity to environmental changes in the humid tropics (Thomas, 2004). They allow the establishment of formal quaternary stratigraphic units (Moura and Mello, 1991; Melo et al., 2001) and a characterization of the responses of landforms to regional expressions of global changes (Servant et al., 1989; Moura et al., 1991; Turcq et al., 1997; Stevaux and Santos, 1998; Modenesi-Gauttieri, 2000).

However, although colluvial deposits are widely spread features in tropical and subtropical Brazil (Melo and Cuchierato, 2004), direct correlative proxy data is usually scarce (e.g. Turcq et al., 1997), making difficult the definition of relationships between landform evolution, controlling environmental factors and global climatic changes. In addition, due to the main processes at work on slopes, the general scarcity and low resolution of the quaternary continental record (Thomas and Thorp, 1996; Thomas et al., 2001) tend to be enhanced in colluvial mantles, since ephemeral flows usually produce unorganized sediments, preventing sound interpretation (Bertran and Texier, 1999; 71

* Corresponding author. Tel.: +55 48 37218583; fax: +55 48 37219983.
E-mail address: maroliv@cfh.ufsc.br (M.A.T. de Oliveira).

Nemec and Kazanci, 1999, Bertran and Jomelli, 2000; Fard, 2001). In this context, the identification of particularly sensitive terrains and landforms in which climate-driven erosive and sedimentary events may be produced and preserved seems to be crucial (Thomas, 2004).

Due to its territorial dimensions, Brazilian lands are under the influence of several climatic regimes, ranging from equatorial and tropical, to mild subtropical climates. This article presents a study of colluvial and alluvial mantles in southern Brazilian subtropical highlands, where mild climates now predominate. Geomorphologic, stratigraphic, sedimentologic, geochronologic, palynologic, isotopic and micromorphologic data, obtained from three near-valley head sedimentary sequences are presented. Since the study sites are located near valley head areas, the fact that these geomorphic units are effective sources of information for Quaternary interpretation is enhanced (Moura et al., 1991; Dietrich and Dunne, 1993).

2. Setting, material and methods

The study sites are located in the northern highlands of Santa Catarina State, in southern Brazil, in the municipality of Campo Alegre (Fig. 1). Campo Alegre is located in the “São Bento do Sul” Plateau, which is characterized by a rocky, stepped, hilly landscape, strongly influenced by differential weathering and erosion, displaying cuesta-like fronts along the Plateau’s border. Neoproterozoic trachytes, rhyolites and ignimbrites from the Campo Alegre volcano-sedimentary basin compose the local bedrocks (Biondi et al., 2001). Weathering of these rocks gives place to important clay deposits, probably influencing morphogenesis during the Quaternary, as deep alteration mantles are common, together with colluvium and alluvium and soils.

Local altitudes range from 850 to 1200 m a.s.l. and the climate is mesothermic, with relatively temperate summers (Köppen’s Cfb type). The mean annual temperature is about 16.4 °C and mean precipitation varies from 1600 to 1800 mm per year. Tropical and subtropical vegetation coexist in the region, forming the so-called *Araucaria* forest (Mixed Ombrophic Forest). Natural and introduced grasslands are also frequent, with gallery forests extending along hollows and valleys (Oliveira and Pereira, 1998). Preliminary geomorphologic surveys in the area had revealed important quaternary deposits preserved in hollows and valley heads (Oliveira et al., 2001). Colluvium, alluvium and buried peat deposits and soil epipedons bear evidence of local environmental changes, the timing of which embraces, so far, a relatively large span of the Last Glacial Cycle (LGC).

Pedostratigraphic sequences were identified and described in the field (Finkl, 1984). Colluvial and alluvial deposits, interstratified with

buried epipedons and peat horizons, constitute the main features observed. Since the terms “colluvium” and “alluvium” may vary in the literature, they are used here in their broad senses to mean, respectively, detritus transported by various processes on slopes and detrital material transported by streams or rivers. The expression “valley head” is used as an equivalent to “hollow” and “unchanneled valley” to mean topographic convergent areas, upslope of the channel network, in which channelized and unchannelized sediment transport may occur. When slope and stream sediments happen to be mixed in the same site as, for instance, near a valley head environment (Dietrich and Dunne, 1993), they are referred to as colluvial–alluvial deposits.

Sedimentary units and buried epipedons were described according to their color, thickness, geometry, texture and gravel content. Samples were systematically taken from both sediments and soils for several studies. Textural analyses were conducted according to standard procedures (Lima, 2005) and the results were displayed on ternary plots for classification. Muddy samples were classified following Flemming (2000) and samples with important gravel content (more than 5%) were classified according to Folk (1974). In some instances, textural data is displayed as the textural index ($\%_{<2\ \mu\text{m}} \cdot \%_{>10\ \mu\text{m}}$), which expresses a ratio between the relative proportion of grains smaller than 2 μm and those larger than 10 μm . Samples which are mainly composed of weathered lithic fragments, or alterorelicts, were impregnated with polyester resin for analysis under polarizing microscopy (Scholle, 1979; Bullock et al., 1985; Delvigne, 1998). When judged appropriate, analysis between macroscopic and microscopic scales of thin lenses was made with the use of digital images (De Keyser, 1999) obtained from a CanoScan-2710 slide-scanner device.

Soil carbon analysis of buried soil samples (total organic C and ^{13}C) was carried out at the Stable Isotope Laboratory of the Centre for Nuclear Energy in Agriculture (CENA), in Piracicaba, Brazil. The organic carbon results are expressed as a percentage of dry weight. ^{13}C results are expressed as $\delta^{13}\text{C}$ with respect to PDB standard using the conventional δ (‰) notations:

$$\delta^{13}\text{C}(\text{‰}) = \left[\left(R_{\text{sample}} / R_{\text{standard}} \right) - 1 \right] \cdot 1000 \quad (1)$$

where R_{sample} and R_{standard} are the $^{13}\text{C}/^{12}\text{C}$ ratio of the sample and standard, respectively. Analytical precision is $\pm 0.2\text{‰}$ (Pessenda et al., 2004).

Excavated organic deposits were sampled for pollen analysis in two sedimentary sequences. Twenty-four (24) samples of 0.5 cm^3 , at 15 cm intervals along 150 cm and 75 cm core samples were collected in plastic bags and stored under cool (ca. +8 °C) and dark conditions

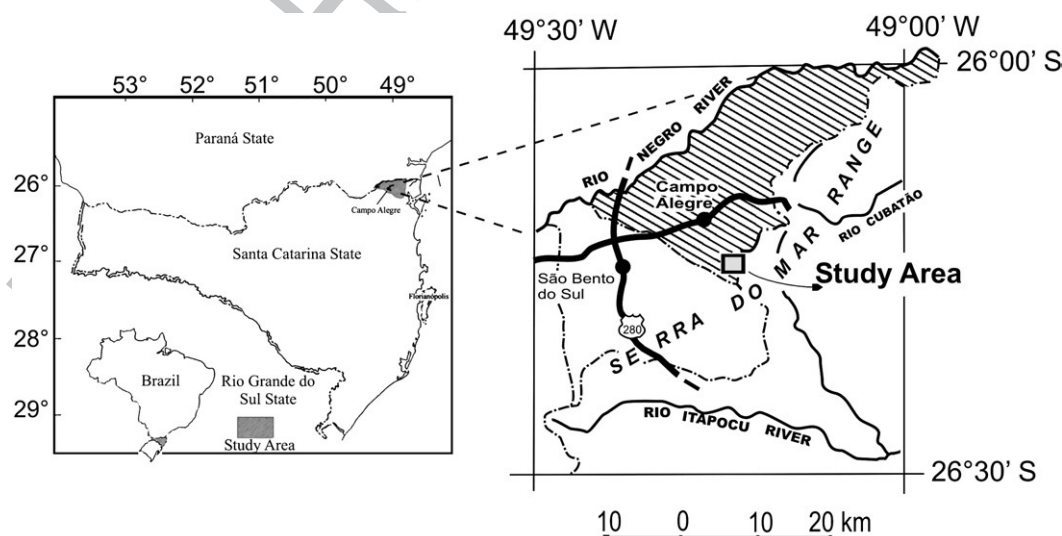


Fig. 1. Study area location.

156 after their return from the field. Samples were processed with stan-
 157 dard pollen analysis methods, using HF (78%) and acetolysis. To
 158 determine the pollen concentration, one tablet of exotic *Lycopodium*
 159 *clavatum* spores was added to each sample. A minimum of 300
 160 pollen grains were counted. For pollen identification, the Behling's
 161 pollen collection was used (containing about 2000 Brazilian species)
 162 together with pollen morphological descriptions (Behling, 1993). For
 163 plotting of the pollen data, calculations and cluster analysis TILIA,
 164 TILIAGRAPH and CONISS software was used (Grimm, 1987).

165 Radiocarbon ages were determined at Beta Analytic Incorporation
 166 (USA); at the Institute of Physics of the Erlangen-Nürnberg
 167 University (Germany) and at ¹⁴C Laboratory of CENA, University of
 168 São Paulo – Piracicaba (Brazil). Thermoluminescence (TL) and optic
 169 stimulated luminescence (OSL) ages were obtained at the Laboratory
 170 of Glasses and Dating from the Faculty of Technology of São Paulo
 171 (FATECSP – Brazil).

172 3. Results and analysis

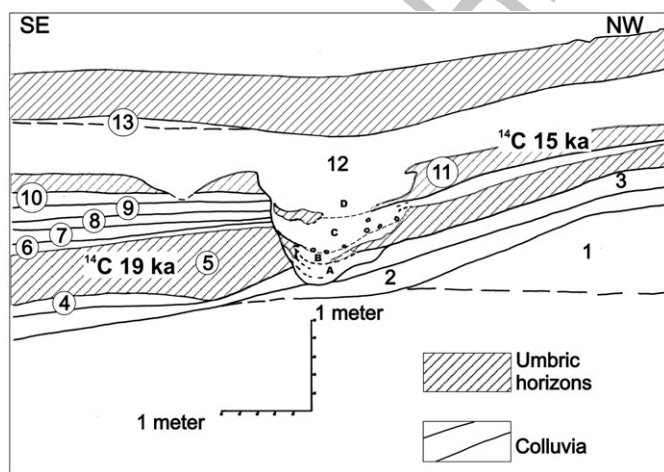
173 3.1. The stratigraphic record

174 Three pedostratigraphic sequences are reported. Distances bet-
 175 ween each sequence vary from about 0.5 to 1.5 km, embracing an area
 176 of approximately 4 km². All reported sequences are located between
 177 the Rio Itapocu river basin and the Rio Negro river basin, in small first
 178 order catchments (see Fig. 1). The Itapocu River flows to the east, along
 179 the local “Serra do Mar” range escarpment, and the Negro River is a
 180 tributary of the Iguaçú River which flows to the west, from the
 181 western flank of the “Serra do Mar” range, entering the Paraná River
 182 and reaching the Atlantic Ocean along the coast of Uruguay and
 183 Argentina, in the “La Plata” estuary. Results are presented according to
 184 the relative increase in distance of each sedimentary sequence from
 185 the drainage divides.

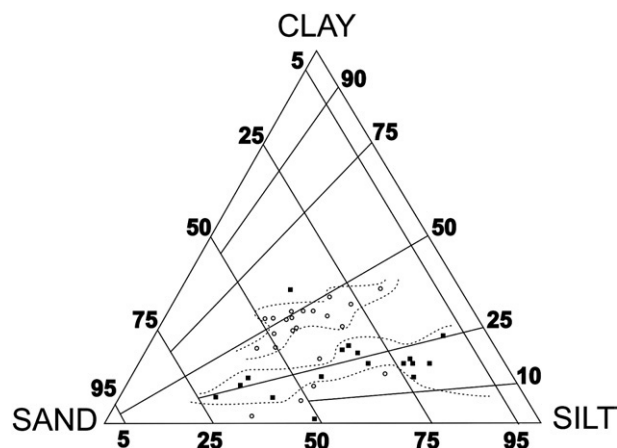
186 3.1.1. Near-divide sedimentary sequence

187 The pedostratigraphic sequence illustrated in Fig. 2 was preserved
 188 near the drainage divides of the so-called “Cerro do Touro” hill, one of
 189 the highest summits in the study area. The sequence is part of a system
 190 of colluvial ramps, which remain perched over a dissected first order
 191 valley.

192 Colluvial lenses and layers intercalate with thick buried epipedons
 193 (pedostratigraphic units 5 and 11 of Fig. 2). The sequence is truncated
 194 at the centre of the figure by channel-like features, constituting cut-
 195 and-fill sedimentary structures, filled by undifferentiated colluvium,



196 Fig. 2. Schematic illustration of the pedostratigraphic sequence, which is located near
 197 the divides. Numbers correspond to main sedimentary units. Note the apparent increase
 198 in the volume of sediments, which is suggested by the increasing width of the gully
 199 infilling sets (A, B, C, D) upwards.



200 Fig. 3. Distribution of samples in the Flemming diagram. Squares indicate samples from
 201 buried epipedons. Circles indicate colluvial samples. Different genetic materials tend to
 202 cluster in different zones of the diagram.

203 the geometry of which follows the present topography. The sequence
 204 ends up with the present-day thick umbric epipedon at the top.
 205 Textural classification of materials from this section may be observed
 206 in Fig. 3.

207 As expected, different materials tend to distribute along different
 208 zones of the diagram, contributing to faciologic analysis (Flemming,
 209 2000; Oliveira and Lima, 2004). Material from colluvial units are
 210 grouped around the centre of the diagram, while samples under the
 211 influence of pedogenesis are distributed along a wider range of
 212 textural classes, depending on their silt content. Gravel content in
 213 colluvial samples ranges from 4.3% to 12.38%, falling to 0.41% in
 214 samples from the buried palaeosoils.

215 According to radiocarbon ages (Table 1), unit 5 was probably de-
 216 veloped during the Last Glacial Maximum (LGM) and unit 11 during a
 217 period between the LGM and the Holocene. No vegetal remnants were
 218 identified inside these buried epipedons and pollen analysis showed
 219 only degraded pollen grains, precluding pollinic study. The black color
 220 of the horizons (10YR 2/1) and their carbon content indicates buried
 221 umbric epipedons (Lima, 2005). Soil carbon content and $\delta^{13}\text{C}$ soil
 222 carbon content of the set buried soils are displayed below (Fig. 4). $\delta^{13}\text{C}$
 223 values indicate a mixture of C₃ type (trees) and C₄ type (grass) vege-
 224 tation in both palaeosol horizons. These soil organic matter (SOM)
 225 results indicate the presence of herbs and trees, which is typical of the
 226 Brazilian Cerrado/Campos transition.

227 According to the topographic position of the sequence, SOM
 228 analysis suggests that trees and bushes were established near the
 229 water divides of the study site, during the LGM. In addition,
 230 stratigraphy and radiocarbon dates suggest a change of sedimentary
 231 pattern along the sequence. Before and around the LGM, probably
 232 under the influence of diffusive mass movements and low tempera-
 233 tures, colluvial lenses and layers intercalated to thick umbric epi-
 234 pedons (see Fig. 2). After the LGM, evidence suggests that gully erosion
 235 produced cut-and-fill structures that were quickly buried under a
 236 thick colluvial layer. This gully erosion episode took place after ¹⁴C
 237 15,260 ± 80 years BP, probably documenting a change of the site's
 238 239 240

241 Table 1

242 Data for radiocarbon ages of the watershed sequence samples

Laboratory code (#)	Beta-124761	Beta-106474	t1.1
Field code (#)	CA.24-10.A1	CA.S-1	t1.2
Depth of the sample (m)	1.2	2.2	t1.3
Stratigraphic unit	11	5	t1.4
Analysis	AMS	AMS	t1.5
Age (¹⁴ C years BP)	15,260 ± 80	19,130 ± 110	t1.6
$\delta^{13}\text{C}$ (‰)	-25.0	-25.0	t1.7

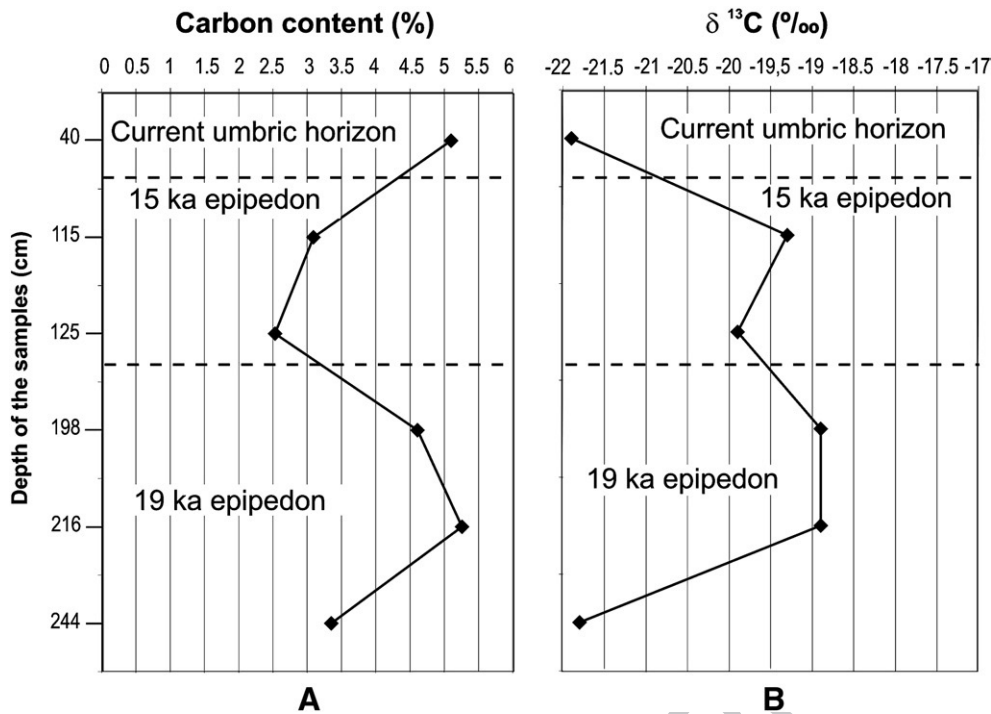


Fig. 4. Soil organic carbon content and $\delta^{13}\text{C}$ values of the watershed site buried soils. Generally, $\delta^{13}\text{C}$ values range from -30 to -22 per thousand for C_3 type plants (trees) and from -17 to -9 for C_4 type ones (grass).

231 hydrologic pattern, passing from diffusive mass movements to
 232 concentrated overland flows. The evident increase in thickness of
 233 the last colluvial layer (unit 12), combined with increasing amounts of
 234 infilling material in the main gully incision (A, B, C, D subunits),
 235 suggest a period of increasing local sedimentation on the slope.

236 3.1.2. Valley head sedimentary sequence

237 The sequence illustrated in Fig. 5 was surveyed at the inner
 238 downslope border of a clay quarry. It represents a typical accretionary
 239 valley head environment, in which episodic erosion and sedimentation
 240 had intercalated with soil development and slow decomposition
 241 of organic matter, under the influence of shallow water-table levels.
 242 Further details on ^{14}C , OSL and TL ages are given in Tables 2 and 3,
 243 respectively.

244 The set begins, at the base, with a 30 to 50 cm thick colluvial
 245 layer composed of sub-parallel lenses of weathered gravels,
 246 displaying subsidiary cross-lamination (unit 1). This unit rests dis-

cordantly over the deeply weathered neoproterozoic pyroclastic
 bedrock and probably dates from an early LGC period (TL 90,000
 $\pm 11,000$ years BP). An abrupt but continual muddy transition above
 led to a buried peat bog, 150 cm thick (unit 2). The ages obtained for
 unit 2 suggests that the upper part of the unit was probably formed
 during marine isotope stage number 3 (MIS 3), while the lower part
 is apparently older than the limit of radiocarbon dating (Tables 2
 and 3).

Unit 2 peat bog is covered by about 1.5 m of undifferentiated mud
 material, strongly altered by hydromorphy (unit 3). The top of this
 hydromorphic unit preserves remnants of a buried ochric epipedon
 truncated by erosion (unit 4) (Fig. 5). A lag deposit composed of well-
 sorted coarse sands is found along the resulting stratigraphic
 disconformity. This sandy deposit was dated by OSL as 6625 ± 260
 750 years old and marks the limit between pleistocenic and
 holocenic sequences at this site. The lag deposit is covered by 75 cm
 of muddy gravel material, displaying normal grading (unit 5). The

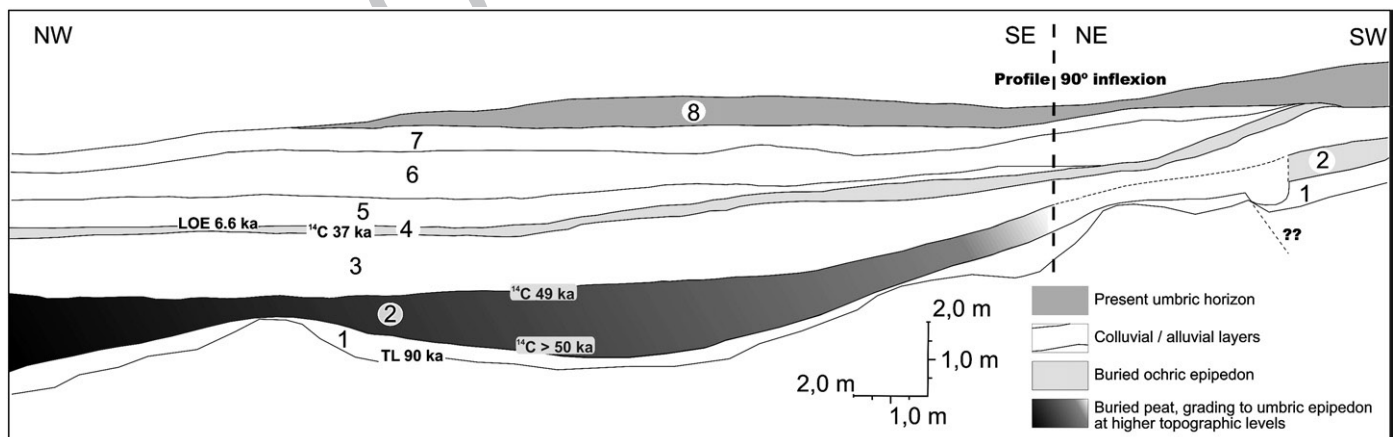


Fig. 5. Schematic representation of the valley head pedostratigraphic sequence. The numbers correspond to main sedimentary units. Note the general concave geometry of the lower sedimentary units and the general convexity of the upper ones.

t2.1 **Table 2**
Data for radiocarbon ages of the valley head sequence samples

t2.2	Laboratory code (#)	# 953/CENA # 520	# 851/CENA # 444	Erl-5456
t2.3	Field code (#)	Paleo-2	CA-TOPO	PH-09/02-2
t2.4	Depth of the sample (m)	2.5	5.4	6.9
t2.5	Stratigraphic unit	4	2 (top)	2 (base)
t2.6	Analysis	AMS	Radiometric	AMS
t2.7	Age (^{14}C years BP)	37,000 ± 1425	49,300 ± 9700–4250	>50,000
t2.8	$\delta^{13}\text{C}$ (‰)	–19.5	–29.0	–28.82
t2.9				

264 sedimentary set terminates with 2.5 m of very-finely-stratified
265 colluvium, made up of alternated lenses of weathered gravel, sand
266 and silt sized particles (units 6 and 7). The dates obtained allow
267 dividing the sequence into two different sub-sequences, the first from
268 the Pleistocene (units 1, 2, 3 and 4) and the second from the Holocene
269 (units 5, 6, 7 and 8).

270 **3.1.2.1. Results from the pleistocenic units.** Detailed textural analysis
271 was performed on samples of units 2, 3, 4 and 6. The buried peat
272 deposit (unit 2) was subjected to detailed sedimentologic and
273 palynologic investigation. Textural classification of unit 2 materials
274 is illustrated in Fig. 6. Viewed as a whole, samples of unit 2 may be
275 grouped in two separate levels: an inferior, texturally coarser level and
276 a superior, texturally finer level, as illustrated in Fig. 7. The two textural
277 levels are separated at a depth of approximately 590 cm by a strong
278 enrichment in clay-sized material.

279 The summary pollen percentage diagram of a core taken from
280 this peat layer (unit 2), including pollen concentration and the
281 cluster analysis dendrogram, shows that the pollen diagram also can
282 be divided into two local pollen zones: respectively, zone I and zone
283 II (Fig. 8). The pollen percentage diagram shows the major
284 significant taxa based on the total pollen sum (Fig. 9). Identified
285 pollen taxa were grouped into Campos, *Araucaria* forest and Atlantic
286 rain forest.

287 Pollen zone I (150–45 cm, 11 samples) is characterized by abundant
288 Campos (grassland) pollen taxa (60–67%), primarily Poaceae, followed
289 by Cyperaceae, *Baccharis*, and Asteraceae subf. Asterioideae and other
290 taxa such as Apiaceae, *Eryngium* and *Valeriana*, which occur in lower
291 percentages. *Araucaria* Forest pollen sums are moderate (25–32%),
292 represented primarily by Myrtaceae, followed by *Podocarpus*, *Wein-*
293 *mannia*, Melastomataceae, *Myrsine*, *Ilex*, *Symplocos* and *Daphnopsis*.
294 Pollen grains of *Araucaria angustifolia*, except one single grain, are
295 missing. Percentages of Atlantic Rain Forest pollen taxa are low (1–3%)
296 and represented only by single grains such as *Alchornea*, *Celtis* and
297 Moraceae/Urticaceae. Aquatic pollen taxa are absent or were found
298 only in single grains. Tree fern spores of *Cyathea* and *Dicksonia* are
299 recorded in low percentages. Other fern spores are more frequent,
300 primarily represented by the *Blechnum imperiale*-type and monlete
301 psilate spores. Percentages of moss spore are rare.

302 In pollen zone II (45–0 cm, 5 samples) pollen grains represent the
303 Campos vegetation, which are continuously predominant along the
304 sequence (60–70%). Percentages of *Eryngium* and some other Campos
305 pollen taxa are somewhat lower, while other taxa remain unchanged.
306 The sum of the *Araucaria* Forest group is similar to zone I, but the

t3.1 **Table 3**
Data for luminescence ages of the valley head sequence samples

t3.2	Laboratory code (#)	LVD-1127	LVD-662
t3.3	Field code (#)	CA-base-LOE	CA-SC-73
t3.4	Depth of the sample (m)	3.4	7.5
t3.5	Stratigraphic unit	Lag deposit	1 (base)
t3.6	Dating method	OSL	TL
t3.7	Annual dose ($\mu\text{Gy/yr}$)	436 ± 40	1800 ± 40
t3.8	P (Gy)	2.89	150
t3.9	Age (years)	6625 ± 750	90,000 ± 11,000
t3.10			

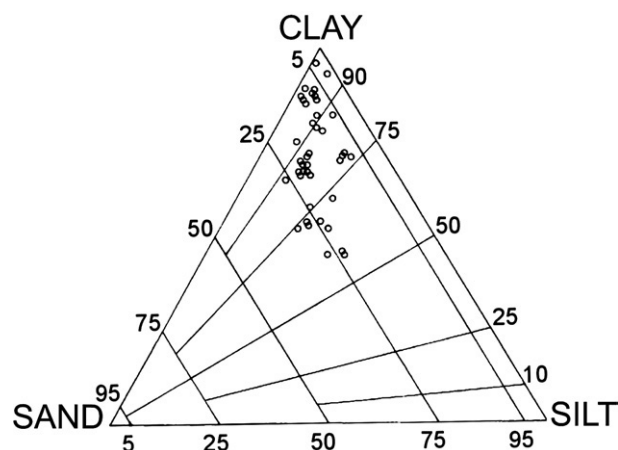


Fig. 6. Flemming textural classification of materials from unit 2 buried peat bog. Most of the peat material is characterized as Flemming type sandy mud (50 to 75% of mud), slightly sandy mud (75–95% of mud) and mud (>95% of mud).

307 composition changed, as Myrtaceae percentage is slightly lower than
308 in zone I, and percentages of *Podocarpus* are markedly higher. Also,
309 percentages of *Weinmannia* became rare. Percentages of the group of
310 Atlantic Forest taxa remain at low levels (1–2%), but pollen of
311 Melastomataceae/Combretaceae decreases, while *Myrsine* increases.
312 Tree fern spores and the *Blechnum imperiale*-type decrease in this
313 zone.

314 This pollen record suggests a change in composition along unit 2
315 from an older period of relatively drier and warmer climate (pollen
316 zone I), to a younger period of wetter and colder climate (pollen
317 zone II). This inference is based on the higher percentages of *Podo-*
318 *carpus* and the rare occurrence of *Weinmannia* in the younger pollen
319 zone II. Indeed, *Podocarpus* needs relatively wet environment for
320 growth and *Weinmannia* would be sensitive to lower LGC tempera-
321 tures (Behling, 1993).

322 The $\delta^{13}\text{C}$ analysis of unit 2 suggests the predominance of tree
323 species, or C_3 type grasses as Cyperaceae, along the entire unit (Fig. 10).
324 Total carbon content decreases continuously from the base to the top
325 of the profile. The association of C_3 grasses and trees in unit 2, the age
326 of which coincides at least with MIS 3, may be explained either as a
327 consequence of early MIS 3 general interstadial trend, or as a
328 consequence of the local concave topography of the buried valley
329 head, making a transitive environment between grasslands in the
330 summits and gallery forests in the valleys.

331 Units 3 and 4 are mainly constituted by material classified as
332 clayey slightly sandy mud, suggesting an apparent low energy envi-
333 ronment for deposition of unit 3. Unit 4 radiocarbon age indicates
334 that this soil epipedon had developed by the end of MIS 3 (Table 2).
335 SOM data obtained from this unit is also displayed in Fig. 10, where
336 more enriched $\delta^{13}\text{C}$ values indicate the presence of less dense
337 vegetation, probably with C_4 type herbs increasing in importance.
338 Globally, SOM results coincide with pollen data (Figs. 8 and 9),
339 suggesting the predominance of a relatively wet local climate
340 condition during the formation of the LGC peat bog (unit 2), which
341 was followed by a relatively local climatic degradation, probably due
342 to increasing dryness, leading to the formation of unit 3 altered
343 muddy material and to unit 4 ochric epipedon, usually formed under
344 warmer conditions in Brazil.

345 These results suggest that periods of erosion and sedimentation
346 had alternated with periods of soil development, in a local environ-
347 ment where a shallow water table gave rise to peat accumulation,
348 slow deposition and hydromorphic weathering. This local soil
349 saturated pedoclimatic condition had probably prevailed during the
350 early MIS 3 interstadial, by the end of which deposits and soils of unit
351 3 and 4, together with SOM data, bear evidence of increasing dryness.

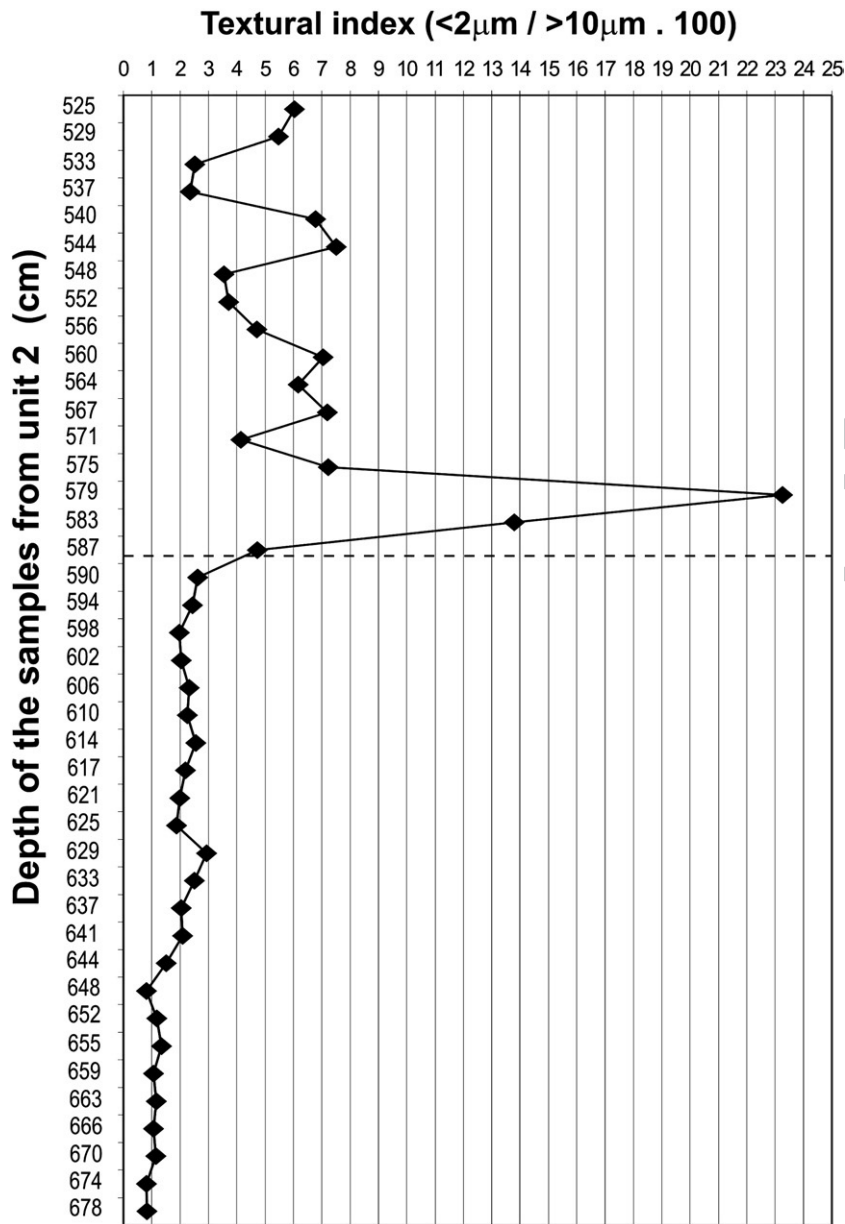


Fig. 7. Grain size ratio ($<2\mu\text{m} / >10\mu\text{m}$) estimated at 5 cm intervals for the 150 cm long peat bog.

352 3.1.2.2. Results from the holocene units. The beginning of the set
 353 holocene sequence is marked by the erosive discontinuity over the unit
 354 4 ochric epipedon. LOE dating of the lag deposit along the discontinuity
 355 suggests that unit 4 was truncated by erosion during the Mid Holocene
 356 (see Table 3). The first deposit over the erosive discontinuity is a 75 cm
 357 thick normal graded layer of muddy gravel (unit 5). This layer is covered
 358 by about 2.5 m of finely stratified colluvial/alluvial material composed
 359 of alternated lenses of gravel, sand and mud (units 6 and 7) (see Fig. 5).
 360 Since clasts of these layers are completely weathered, forming loose
 361 alterorelicts (*sensu* Delvigne, 1998), their textural analysis was con-
 362 ducted by optic microscopy. Samples from the erosive discontinuity
 363 and from units 5 and 6 were analyzed.

364 Results of the micromorphologic analysis of samples from this
 365 transition and from samples of unit 5 and 6 suggest: a) shearing near
 366 the top of the buried truncated epipedon (unit 4); b) relatively rapid
 367 local burying, following erosion of unit 4; c) carbonized small roots in
 368 pedotubules of unit 4; d) clastic deposition inside unit 4 cracks and e)
 369 post-depositional weathering of overlaying units (units 5 and 6)
 370 (Oliveira et al., in press).

Unit 6 is composed of alternated lenses of mud and gravel. If 371
 plotted in ternary diagrams for textural classification, the muddy 372
 subunits would be classified as Flemming's clayey sandy mud (C–V) 373
 and very clayey slightly sandy mud (D–V), while the gravelly subunits 374
 would classify as gravelly mud, muddy gravel and gravelly muddy 375
 sand, according to Folk's ternary diagram (Folk, 1974). Fig. 11 illustrates 376
 scanned images of thin lenses obtained from a sample of unit 6 (Fig. 377
 11A) and from one sample of contemporary rain-wash deposits (Fig. 378
 11B). The latter was created over the bare floor of the study site clay 379
 quarry (Fig. 12), about 50 m from the pedostratigraphic sequence, after 380
 three days of rain, amounting to about 59.7 mm. Clastic material from 381
 holocene and contemporary deposits of Fig. 11 seem to come from the 382
 same source area. 383

A comparison of the scanned thin lenses shows similar structures, 384
 although some important differences may be noted (Table 4). 385
 Alternation of coarse and fine lamina is common in both holocene 386
 and contemporary samples. Inner detailed structures show that the 387
 holocene sample (Fig. 11A) is mainly composed of discrete massive 388
 and compacted lamina of mud, sands and gravel, since 67% of the 389

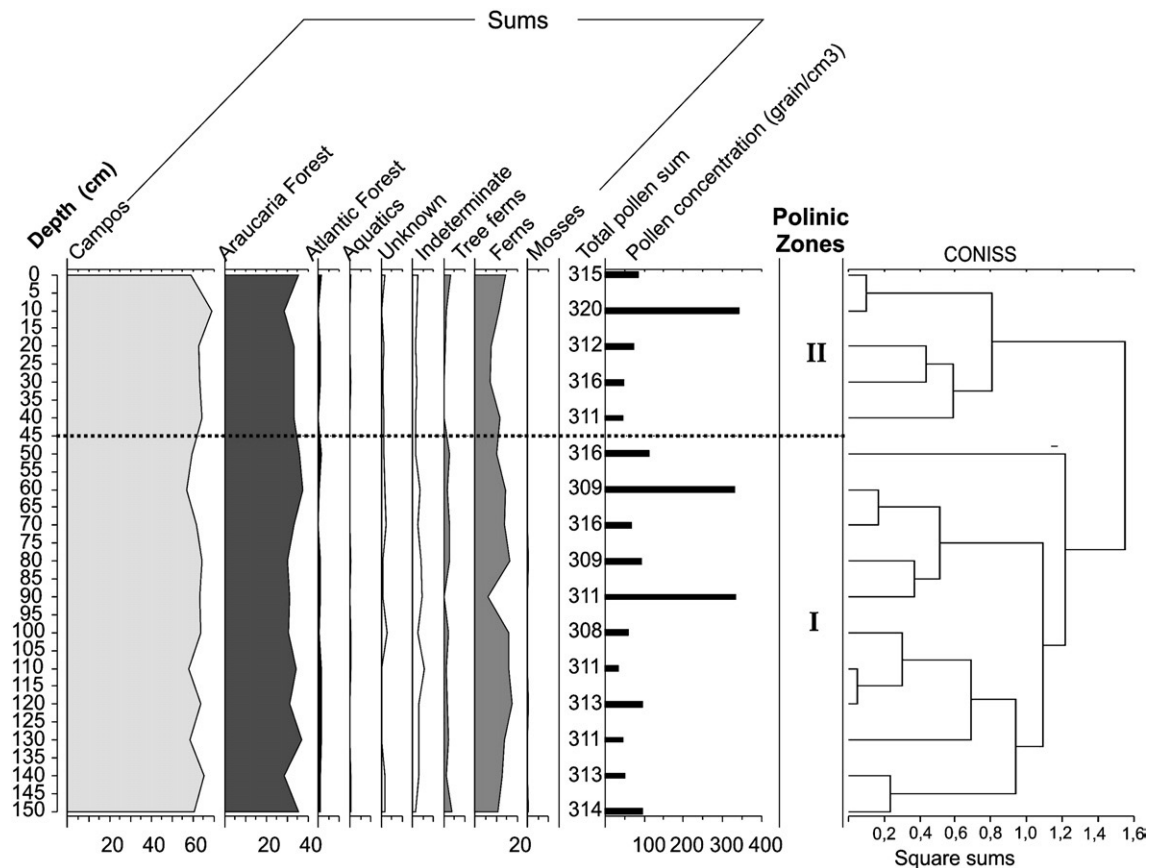


Fig. 8. Summary pollen percentage diagram, including pollen concentration and the cluster analysis dendrogram, of the buried peat bog.

390 laminae are massive (units 1, 2, 3, 4, 6, 9', 10, 11), while 33% display
 391 preferential organization (units 5, 7, 8, 9) (Table 4). The present-day
 392 rain-wash sample (Fig. 11B) has 53% of massive lamina (units 1, 2, 3, 4,
 393 7, 8, 13), while 47% are better organized (units 5, 6, 10, 10', 11, 12, 14)
 394 (Table 4). Massive and preferentially organized lamina in the
 395 contemporary sample present a more openly-packed framework
 396 structure, mainly composed of sand, gravel and some mud.

397 The geometry of lamina in both samples shows that fine gravel and
 398 coarse sand compose lenticular bodies, while fine sand and mud tend
 399 to make parallel-sided lamina (Fig. 11), eventually developing inner
 400 lamination, clearly visible under microscopy. The holocenic deposit
 401 displays better sorting and better inner organization in finer
 402 sediments (fine sands and mud), while poor sorting and massive
 403 lenses are mainly made by coarser sediments (Table 4). The
 404 contemporary deposit does not display any clear textural relationship,
 405 in spite of a tendency to improve inner organization in the lower mode
 406 matrix-supported lamina (Table 4).

407 The two samples have a similar geometry of coarse and fine
 408 lamina and lenses. In general, the inner organization is quite similar,
 409 although a slight majority of massive lamina is observed in the
 410 holocenic sample. In spite of this, the holocenic lamina have a strong
 411 correlation between grain size and sorting ($r=0.72$), while the
 412 contemporary lamina display no significant correlation between
 413 textural characteristics (Table 4). In addition, the holocenic lamina
 414 are slightly better sorted than the contemporary ones (67% of
 415 holocenic and 60% of contemporary lamina classify as well to very
 416 well sorted sediments).

417 Little doubt exists about the origin of the contemporary deposit,
 418 since it is the fresh result of rain-washing flows, witnessed in the field
 419 (Fig. 12). Concerning the holocenic deposit, if we take into account,
 420 first, its depositional setting (an unchanneled swale); second, the
 421 general structural similarities between coarse and fine lamina in

422 holocenic and contemporary samples; third, the general description
 423 of the holocenic deposits at the stratigraphic section, we must
 424 suggest: a) that both contemporary and holocenic deposits are
 425 typically slope wash deposits; b) that rain-washing flow is the main
 426 depositional agent in both cases (Oliveira et al., in press). This
 427 suggestion is also supported by the differences between the two
 428 samples: a) the pluvial contemporary deposit is better organized,
 429 although poorly sorted, probably due to the continuous variation of
 430 precipitation rates during the three rainy days recorded, leading to
 431 mechanical sieving and impregnation of coarser sediments by finer
 432 ones, during lowering flow rates (Ferreira and Oliveira, 2006); b) the
 433 torrential holocenic deposit is mainly massive, although better
 434 sorted, suggesting sporadic variable pulses of precipitation with
 435 rapid deposition, which are characteristic of drier environments.
 436 Indeed, massive, parallel laminated and graded sandy laminae are all
 437 indicative of depositional processes associated with fluctuations of
 438 fluid flow strength. Massive and laminated sands, which predominate
 439 in the holocenic sample, indicate rapid deposition, while grading,
 440 more frequent in the contemporary sample, is usually associated with
 441 fluctuations in flow energy. Considering this evidence, general and
 442 detailed structures found in the holocenic Unit 6, of this valley head
 443 sequence, suggest that the holocenic units were formed in an alluvial
 444 fan-like setting, during the early to mid Holocene, under the in-
 445 fluence of rain-washing flow.

446 As a result, the holocenic sequence reveals deposits that had
 447 probably formed under the influence of pulses of rain-washing over
 448 the adjacent slopes of the study valley head, implying local footslope
 449 aggradation in a sedimentary setting that was probably marked by
 450 long dry seasons during the mid Holocene. Indeed, relative dryness is
 451 required to explain such deposits, since it causes the necessary
 452 rarefaction of vegetation for rain-washing flows over relatively bare
 453 slope surfaces, building up alluvial fan structures (see Fig. 12).

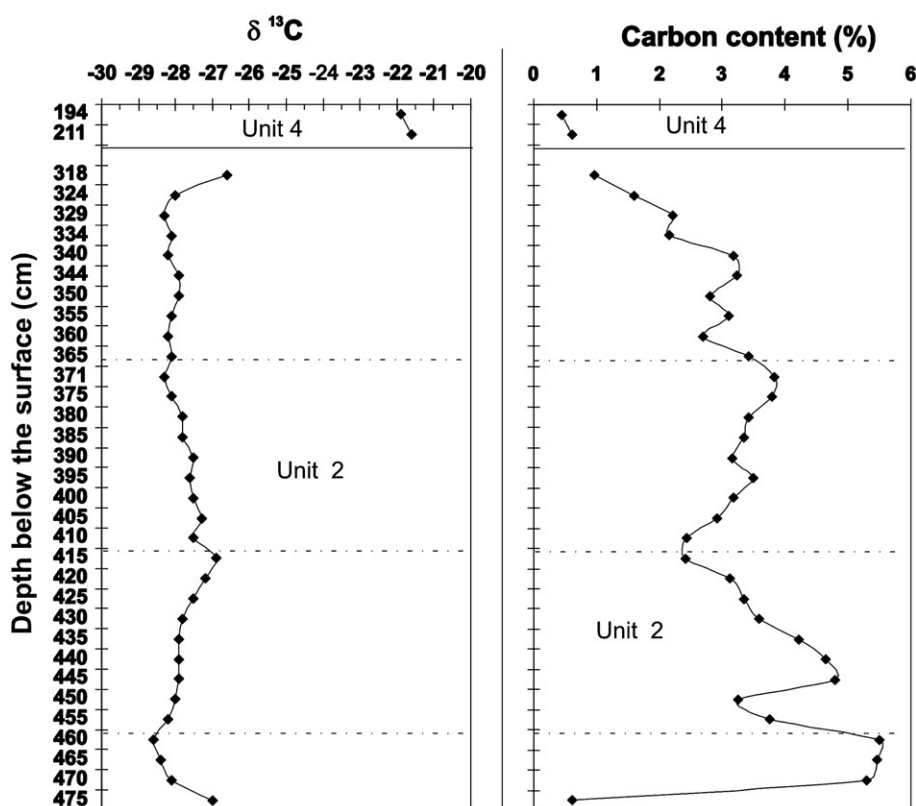


Fig. 10. $\delta^{13}\text{C}$ soil carbon values and organic carbon content of unit 2 site buried peat in the valley head sedimentary sequence. Generally, $\delta^{13}\text{C}$ values range from -30 to -22 per thousand for C_3 type plants (trees) and from -17 to -9 for C_4 type ones (grass).

3.1.3. Valley bottom sedimentary sequence

The sedimentary sequence is located about 700 m downslope from the near-divide study site (see Section 3.1.1 above), and pertains to the same drainage system. The sequence was built up in an alluvial fill, at a reach where the deep incised first order valley widens, upslope from a local rocky base level. As suggested by Fig. 13, the sedimentary sequence looks like a typical floodplain deposit with alternating channel fill sands and overbank mud (Miall, 1985).

The sequence begins with a colluvial layer, set over one of the side-slopes of the valley floor (unit 1). An undated umbric epipedon evolved over this layer (unit 2) (Lima, 2005), before it was buried under a second colluvial layer (unit 3). Erosion of colluvia, soil and valley floor probably preceded deposition of the sandy and gravel onlapping alluvial lenses of units 4 and 5. The unit 5 gravel layer preserves plant material inside, resting discordantly over the previous units. A peat deposit was developed over these gravels (unit 6), which

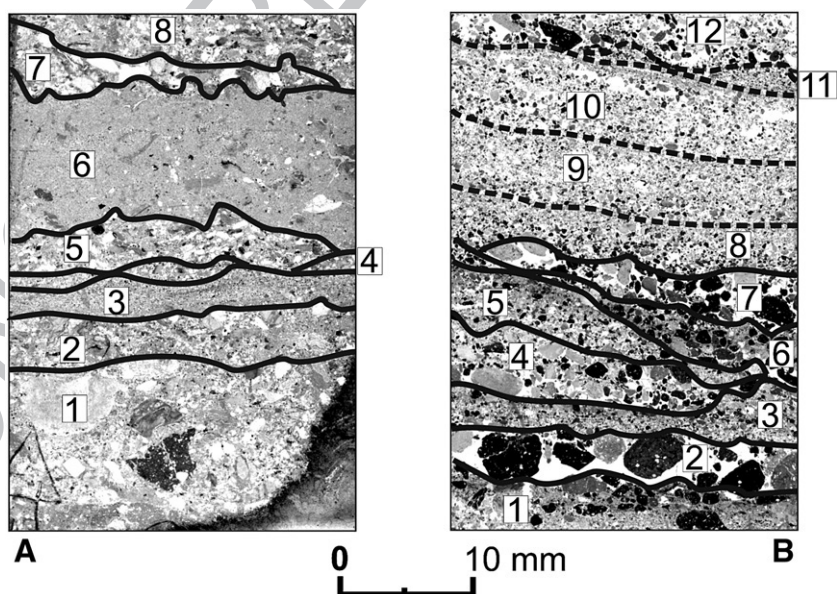


Fig. 11. Scanned images obtained from thin sections of Quaternary (A) and contemporary (B) deposits. Images were taken under transmitted light. Numbers indicate the sedimentary units, the transition of which is emphasized by drawing lines. Note glebule (G) at the base of unit 2, in (A), which actually is a fragment of soil aggregate, indicating that the deposit was associated with soil erosion.



Fig. 12. Sedimentary pattern of a slope wash deposit, created along the floor of the study clay quarry, after a 60 mm rain event. The deposit was located upslope of the valley head pedomorphological sequence, about 50 m away.

was partially truncated by erosion, probably in association with the deposition of a channel fill (unit 7), marking the beginning of the floodplain deposits. A series of overbank clayey and silty deposits follows (units 8, 10, 12, 13, 15, 16 and 17), alternated with sandy lenses (units 9, 11 and 14). Unit 18 is the current epipedon, which is already partially buried under a thin and discontinuous layer of colluvium from the adjacent side-slope (unit 19). Further details on ^{14}C and TL ages obtained from materials of the sequence are given in Tables 5 and 6 respectively.

The textural classification of materials in the sequence is illustrated in Fig. 14. Most of the deposit is composed of muddy material. Overbank sediments and buried epipedons range from Flemming textural types, slightly sandy mud (D) to mud (E), while channel fill sediments range from sandy mud (C) to muddy sand (B), plotting in different domains of the diagram. The gravel content of sediments varies from 10% to 50% in colluvial samples and does not exceed 5% in alluvial samples. There is no SOM analysis for material from the sequence.

A core of the buried peat layer (unit 6) was studied by pollen analysis. The summary pollen percentage diagram of the core can be divided into two local pollen zones, zone 1 and zone 2 (Fig. 15).

Pollen zone 1 (223–188 cm, 4 samples) is characterized by abundant Campos (grassland) pollen taxa (70–85%), primarily Poaceae, followed by Cyperaceae, Asteraceae subf., Asteroideae and *Baccharis*. *Araucaria* Forest pollen sums are moderate (10–20%), represented primarily by Melastomataceae and *Myrsine*, followed by *Weinmannia* and Myrtaceae. Pollen grains of *Araucaria angustifolia* are missing. The representation of Atlantic Forest pollen taxa are low (1–3%) with some single grains such as *Alchornea* and Moraceae/Urticaceae. Tree fern

spores of *Cyathea* and *Dicksonia* are recorded in low percentages. Other fern spores are more frequent, primarily represented by the *Blechnum imperiale*-type and monolete psilate spores.

In pollen zone 2 (188–152 cm, 4 samples) pollen of the Campos vegetation are still frequent (50–60%), but markedly less so than in zone 1. Percentages of Poaceae decrease while Cyperaceae percentages increase at the top of the core. Other Campos pollen taxa remain unchanged. The sum of the *Araucaria* Forest group increase, especially by Myrtaceae and *Weinmannia*. Also, other *Araucaria* Forest taxa appear, such as the *Lamanonia speciosa*-type, *Clethra*, the *Symplocos tenuifolia*-type and *S. lanceolata*-type. Percentages of the group of Atlantic rain forest taxa remain at low levels (1–2%). Ferns such as *Blechnum imperiale*-type decrease in this zone, while tree fern *Dicksonia sellowiana* and Monolete psilate percentages increase, followed by *Cyathea* and Trilete psilate types.

This Late-glacial age pollen record suggests a change from an older period with a relatively dry and cold climate (pollen zone 1), before ^{14}C 11.8 ky, to a younger period with a wetter and warmer climate (pollen zone 2), ending at ^{14}C 11.3 ky. This is reflected by a change from Campos with some gallery forest towards larger areas of *Araucaria* forest, mainly in the form of gallery forest along the valley. The general expansion of the gallery forest, the increase of tree ferns such as *Dicksonia sellowiana* and *Weinmannia* trees also indicates wetter and warmer conditions during the pollen zone 2 period. Since the top of the deposit is missing, probably truncated by erosion before burial, no further conjecture is possible at this time.

Globally, this first order valley sequence bears evidence of shallow braided channel sedimentation around TL 86 ky. This LGC deposit was covered by peat, formed in a shallow swampy environment at the valley bottom, at least around the Late Pleistocene ($>^{14}\text{C}$ 11.8 ky BP to ^{14}C 11.3 ky BP). Radiocarbon ages, together with pollen record, indicate a relatively rapid change in vegetation composition, in about 500 years, which coincides with the end of the northern hemisphere's Younger Dryas. The peat deposit was partially truncated and covered by undated overbank deposits characteristic of single thread channels, suggesting a switch from an earlier braided system, passing from a swampy environment, to a low-energy fluvial single thread system.

3.2. Stratigraphic correlation

Based on measured ages, the different pedomorphological sequences were superposed in a graphic sedimentary log (Fig. 16) that presents the maximum thickness of the main layers at each site, as well as their general characteristics. Organized as such, the study deposits may be divided in three different sequences: Lower Sequence, Intermediate Sequence and Upper Sequence.

As suggested by Fig. 16, the study ages coincide with a relatively wide LGC time span, embracing several recognized climatic events in both hemispheres, such as marine isotopic stages (MIS 5, MIS 3, MIS 2 and MIS 1), substages (5c, 5b, 5a), millennial oscillations on climate improvement periods (Bølling/Allerød interstadials; warming trend before Antarctic Cold Reversal) and Late Pleistocene events (Younger Dryas) (Bond et al., 1993; Blunier et al., 1998; Blunier and Brooks, 2001; Cortese and Abelmann, 2002). The study record is truncated, as usual, and one radiocarbon age is technically ambiguous, but the

Table 4
Data for radiocarbon ages of valley bottom sequence samples

Laboratory code (#)	Beta 203292	t4.2
Field code (#)	NE-F6-AM16	t4.4
Depth of the sample (m)	1.88	t4.5
Stratigraphic unit	6 (Middle)	t4.6
Analysis	Radiometric	t4.7
Age (^{14}C years BP)	11,850 ± 70	t4.8
$\delta^{13}\text{C}$ (‰)	-18.8	t4.9

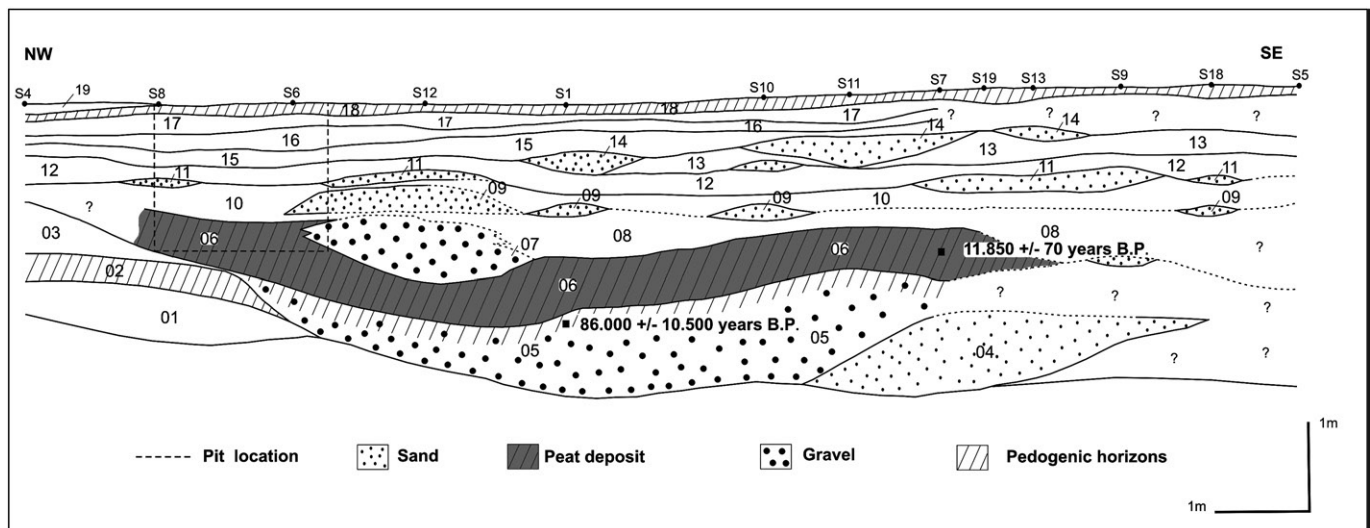


Fig. 13. Schematic representation of the valley bottom pedostratigraphic sequence. Numbers correspond to main sedimentary units. The sequence was surveyed by manual drillings. One pit was excavated for sampling and to check detailed structures.

552 sedimentary source-to sink pathway of the study near-valley head
553 sites is definitely short and coincidences seem consistent. In addition,
554 independent radiocarbon and luminescence ages reported for all three
555 Southern Brazilian States (Paraná; Santa Catarina; Rio Grande do Sul)
556 also suggest the likeliness of a regional signal in Southern Brazil (Fig.
557 17), probably linking erosive and sedimentary events to global and
558 hemispheric climatic trends, which could be summarized as follows,
559 according to Fig. 16 idealized sedimentary sequence.

560 3.2.1. The Lower Sequence

561 a) About TL 90 ky to 86 ky: erosion of weathered mantles and
562 deposition of gravels with subsidiary cross-lamination on slopes and
563 adjacent valleys. Correlative global and hemispheric events: MIS 5b
564 stadial (N.H.) and change from interstadial to stadial condition (S.H.)
565 (Aharon and Chappell, 1986; Cortese and Abelmann, 2002). Possible
566 scenario: erosion and deposition by rain-washing and flash floods in
567 slopes and valleys, during stadial transition. b) About ^{14}C 49 ky BP, or
568 earlier (>50 ky): peat development and proxy evidence (pollen and
569 isotopes) for a relatively wet local environment, with changes in
570 temperature and humidity during the period (from drier and warmer
571 towards wetter and colder). Correlative global and hemispheric
572 events: abrupt climatic oscillations in a longer-term cooling trend;
573 Dansgaard–Oeschger stadials (N.H.) and interstadial oscillations (S.H.)
574 of MIS 3 interstadial (Bond et al., 1993; Peterson et al., 2000; Cortese
575 and Abelmann, 2002). Possible scenario: abrupt changes during a local
576 MIS 3 interstadial that was colder than today, but still humid enough
577 to develop and preserve peat deposits on valley heads. c) About ^{14}C
578 38 ky BP: development of ochric epipedon on valley heads and proxy
579 isotopic evidence of local vegetation rarefaction. Correlative global and
580 hemispheric events: same as above, during MIS 3 (Bond et al., 1993).
581 Possible scenario: although colder than today, relatively warm and dry
582 climate during one of the MIS 3 southern hemisphere interstadial
583 oscillations. The limit between Lower and Intermediate Sequences
584 (Fig. 16) may be determined by the stratigraphic site-discordance
585 created around OSL 6.6 ky, but a causal relationship with any other
586 obliterated erosive or depositional event is not to be discarded.

587 3.2.2. The Intermediate Sequence

588 a) About ^{14}C 19 ky BP: diffusive colluvial deposition; development
589 of thick umbric epipedons and proxy evidence (isotopic) of mixed
590 grasslands and forests (Cerrado) near the study drainage divides.
591 Correlative global event: MIS 2 last glacial maximum (LGM) in both
592 hemispheres (Sowers and Bender, 1995). Possible scenario: morpho-

593 genesis and pedogenesis in a local environment colder and dryer than
594 today, but still humid enough to develop thick umbric epipedons and
595 enable the establishment of trees and bushes around summital areas.
596 b) About ^{14}C 15.3 ky BP: scattered colluviation and umbric epipedon
597 development, followed by a change of local slope hydrology, passing
598 from diffuse mass movements towards gully erosion and cut-and-fill
599 structures. Correlative global and hemispheric events: climatic
600 improvement between MIS 2 and MIS 1; stadial period before the
601 Bølling–Allerød interstadials (N.H.) and warming trend before the
602 Antarctic Cold Reversal Oscillation (S.H.) (Sowers and Bender, 1995;
603 Blunier et al., 1997). Possible scenario: adaptation of hydrogeomorphic
604 systems during period of warming trend (Climatic Improvement),
605 approaching Termination I (Schaefer et al., 2006). c) Between ^{14}C
606 11.8 ky BP and ^{14}C 11.3 ky BP: peat development in a swampy valley
607 environment; proxy pollinic evidence of local climatic change from
608 colder and dry towards warmer and wetter conditions. Correlative
609 global and hemispheric events: end of the Younger Dryas (N.H.), Late
610 Pleistocene oscillations (S.H.) (Broecker, 1995; Sugden et al., 2005).
611 Possible scenario: rapid response of vegetation to climatic ameliora-
612 tion and lower energy depositional environments near the valley
613 heads in a period correlative to the end of N.H. Younger Dryas. There is
614 a gap in the study Intermediate Sequence, between 15.3 ky and 11.3 ky
615 that prevents interpretation about the transition between the Climatic
616 Improvement period and the eventual onset of the Late Pleistocene
617 Younger Dryas. The limit between the Intermediate and Superior
618 Sequences (Fig. 16) may be defined either by the OSL 6.6 ky
619 stratigraphic discontinuity, or by any other erosive event among ^{14}C
620 15.3 ky and ^{14}C 11.3 ky.

621 3.2.3. The Upper Sequence

622 a) About OSL 6.6 ky: soil erosion; sedimentologic and micromor-
623 phologic evidence of dry conditions and wildfires; relatively thick well

Table 5

Data for luminescence age of the valley bottom sequence sample

Laboratory code (#)	LVD-1128	t5.2
Field code (#)	CA-Terraço	t5.3
Depth of the sample (m)	2.4	t5.4
Stratigraphic unit	5	t5.5
Dating method	TL	t5.6
Annual dose ($\mu\text{Gy}/\text{yr}$)	1.150 \pm 26	t5.7
P (Gy)	100	t5.8
Age (years)	86,000 \pm 10,500	t5.9
		t5.10 Q2

Table 6
Comparison between South America LGC events reported by Iriondo (1999) and events deduced from the study sedimentary sequences

Late quaternary stage	Patagonian pattern (P)	Venezuelan pattern (V)	Study highlands pattern
MIS 5	No mention	No mention	Stadial, or stadial transition. Flash floods on slopes and valleys
MIS 4	Cold. Extremely stable dryness	Oscillating cold and warm climates	No mention
MIS 3	Warming climate with 3 major alternated events (humid/dry/humid)	Cold, followed by irregular climatic improvement and glacial events	Colder than today and humid. 3 stratigraphic events (peat; mud deposits; ochric epipedon). Warming and drying to the end of IS.
MIS 2	Similar to MIS 4	Cold and wet before 23 ky. Glacial events between 23 ky and 19.5 ky.	Cold. Although dryer, relatively wet at 19.5 ky.
Climatic improvement	Increasing humidity by 15–16 ky	Lower temperatures and dry climate before 13 ky	Cold, but increasing humidity after 15 ky.
Late Pleistocene (Younger Dryas)	Increasing dryness and torrential events	Warm and humid (12.25 ky–11.96 ky). Cold and humid (11.7 ky–9.51 ky)	Late Glacial conditions (dryer). Change to humid climate at 11.8 ky, with lowering fluvial energy.
Hypsithermal	Warm and humid climate. Floods and	Warm and humid (9.35 ky–6.2 ky).	Increasing dryness. Seasonal regimes and wildfires.

stratified rain-wash deposits on aggrading bare footslopes. Correlative global and hemispheric evidence: Hypsithermal (N.H.); warmer climates, either dry or wet (S.H.) (Iriondo, 1999). Possible scenario: local mid Holocene dryness and a seasonal, contrasted climatic regime.

4. Discussion

4.1. Highland near-valley head climate constraints in Southern Brazil

Since no consistent evidence of local influence of tectonism has come to light so far, the study's near-valley head stratigraphic record seems related to the adaptation by local geomorphic systems to environmental constraints that coincide with global and hemispheric climatic changes. This adaptation to climate-driven factors seems to follow a pattern in which important changes in erosion, sedimentation and pollen taxa production tend to cluster around periods of transition between stadials and interstadials, whatever the sign of the climatic change, although warming periods seem to produce more important geomorphogenic responses. During climatic “steady-state” periods, such as interstadials and stadials, ochric and umbric epipedons and peat deposits formed, in addition to less expressive diffusive colluviation (Fernandes and Dietrich, 1996). This general pattern, if correct, is probably due to local responses of geomorphic systems to changes in the principal South American first-order climatic systems: the ITCZ, the trade-winds and the three oceanic anticyclones: Azores (AA), South Atlantic (SAA) and South Pacific (SPA).

The record of climatic changes in the South American plains between MIS 4 and Little Ice Age was summarized by Iriondo (1999) who identifies the influence of two main climatic pattern types, derived from present-day dynamics of South-American climatic systems. On the basis of previously published data, the author points to an inversed correlated climatic signal between northern and southern South America during Quaternary climatic oscillations. This inversed signal is explained as a consequence of the preponderant influence either of the southern Pampean climatic type pattern (P), or of the northern Venezuelan climatic type pattern (V). Comparison between events reported by Iriondo (1999) and the study events is illustrated by Table 7.

As far as the information reported in Table 7 coincide, events in the study highlands fit better with the Patagonian (P) pattern, in agreement with Iriondo's climatic types distribution in South America (Iriondo, 1999, p. 110), although coincidence seems stronger during irregular oscillating periods (MIS 3, Climatic Improvement, Late Pleistocene–Y.D.). During “steady-state” stages (MIS 2 and Hypsithermal) a mixed Venezuelan (V) pattern seems to preponderate. Generally, these coincidences are coherent with the previously mentioned apparent pattern of adaptation of the study geomorphic systems to climate-driven factors, where periods of transition would lead to morphogenesis while “steady” periods would induce umbric epipedon and peat formation.

The explanation may be controversial, but probably relates to the balancing effects of cold southern air masses and continental or oceanic tropical air masses around the study area (Grimm et al., 2000). The strong South America latitudinal asymmetry, caused by warm ocean waters in the North and cold ocean currents in the South (Iriondo, 1999), would tend to reinforce effects of regional temperature gradients during irregular oscillating periods, or transitions, enabling expansion of the Patagonian (P) pattern to lower latitudes, either as a result of spreading colder and denser southern air masses, or as a consequence of weakening SAA influence. Tropical continental and oceanic air masses would tend to increase in influence during “steady-state” periods, either cold or warm, pushing the Venezuelan climatic pattern (V) southwards.

Reported results from the Cariaco Basin, off the Venezuelan coast, suggest that increased precipitation and river discharges are closely linked to MIS 3 interstadial abrupt shifts, as recorded in Greenland ice cores (Peterson et al., 2000). This would also suggest that northern South America climatic changes would be synchronous to the northern hemisphere's major climatic changes, emphasizing the existence of far-reaching teleconnection effects that link Milankovich's “sensitive latitudes” to equatorial climate, or vice-versa. Evidence of a mixed Venezuelan “V” pattern at the study LGM and MIS 1 record, during “steady state” periods, may be viewed as another example of the teleconnection hypothesis. However, the reasons why the study record suggests an extending influence of the “V” pattern climate to areas where the “P” pattern would be expected (Iriondo, 1999) are still not clear enough for further conjecture.

Iriondo's bi-polar model also predicts local transient climatic conditions. Concerning the study area, these local conditions may be

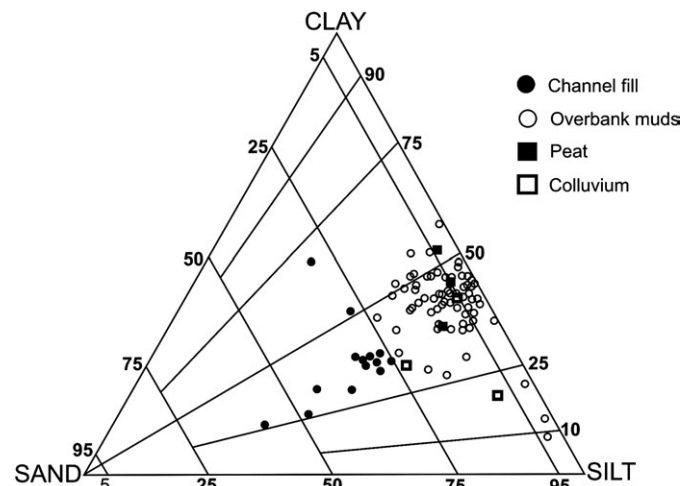


Fig. 14. Flemming textural classification of materials from the valley bottom sedimentary sequence. Different genetic deposits tend to cluster in different zones.

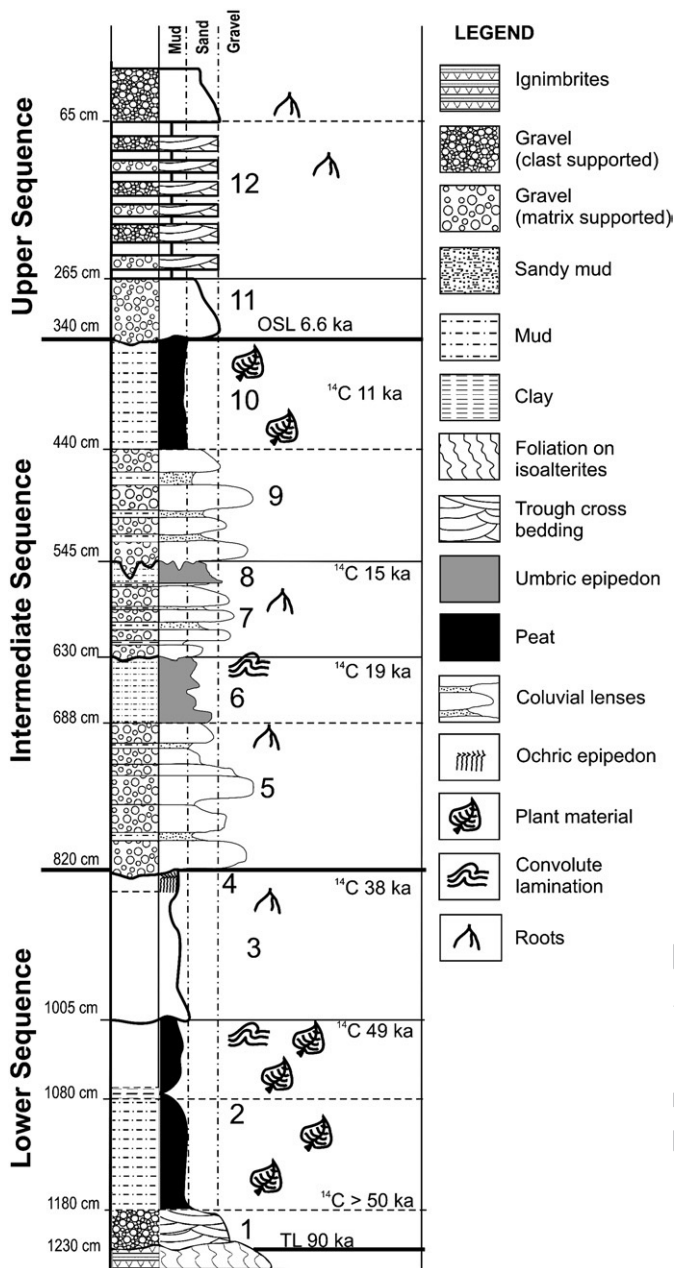


Fig. 16. Idealized sedimentary log of all study pedostratigraphic sequence's deposits. The numbers indicate the main sedimentary units, ordered by their age.

important, since the sites locate near the watersheds, about 1000 m a.s.l., in valley heads of very small catchments, perched between the steep Atlantic *Serra do Mar* ranges and the gentle westerly dipping Southern Brazilian Plateau highlands. Under these circumstances, Atlantic Polar Cold Front migration and local orographic effects may be equally important controlling factors, influencing the response of hydrogeomorphic systems. This is probably the case for the evidence found in this study of dryness during the mid Holocene, as well as for the relatively wet conditions during MIS 3 and LGM.

Independent interpretation for the "Serra Campos Gerais" pollen record had suggested a Holocene palaeoclimate with a long dry season (Behling, 1997a). This may also have been the case for the study sites, where no annual dry season occurs under modern climatic conditions. This climatic condition with a marked seasonal dry period in early and mid Holocene could be explained by a stronger influence from dry, tropical continental air masses in Southern Brazil (Behling, 1993), which would have blocked polar cold fronts farther south preventing

precipitation over the study area. Evidence of longer dry seasons in the early Holocene were also found in different records from S and SE Brazil (Servant et al., 1989; Behling, 1997b; Pessenda et al., 2004; Melo and Cuchierato, 2004; Moro et al., 2004), suggesting a regional trend which points to possible future local effects of current global climatic warming. In addition, according to models run by Wasson and Claussen (2002) this relative early-mid Holocene dryness would be expected to occur in Australia and Africa, at similar latitudes, and even at lower ones, as suggested by the short arid pulses depicted by high-amplitude lake regressions in the main Ethiopian rift during the period (Benvenuti et al., 2002).

The chronology of the study near-valley head stratigraphic record is coincident with global and hemispheric events depicted in Greenland and Antarctic ice caps (Bard et al., 1997; Blunier et al., 1998; Blunier and Brooks, 2001; Clark et al., 2002; Weaver et al., 2003). Conjecture about major regional climatic factors may explain why transitions between stadial and interstadial periods seem to be associated with erosion and rain-wash deposition in the study slopes and valleys, probably under the influence of contrasted seasonal climatic regimes. Organic-rich soils and peat deposits, which need conditions of water saturation for several months to fully develop (Shoty, 1992), are present in every sequence of the study. Their ages coincide with LGC periods when global temperature was lower than today, which is also supported by the study proxy data, suggesting the existence of shallow soil-water saturated zones in topographic hollows under the influence of local wet environments, low temperatures and low evaporation rates. This local wet soil-environment condition would tend to maintain overland flow as an efficient and recurrent mechanism through time, also explaining the dynamics of alternate periods of pedogenesis and morphogenesis at the study valley heads, implying anaerobic soil development during climatic stable periods and soil erosion and local deposition under transient climate conditions.

5. Conclusions

The study sites witness an important LGC stratigraphic record which give evidence of the adaptation of near-valley head areas to climate-driven processes in the humid tropics. Due to their relative scarcity in Quaternary colluvial-alluvial stratigraphy studies, a number of results deserve mention: a) evidence of erosion and sedimentation at early LGC stages; b) evidence of sedimentation and pedogenesis during the LGM; c) evidence of hydrogeomorphic changes during the Climatic Improvement, between MIS 2 and MIS 1; d) sedimentary evidence of pronounced dryness, at least under contrasted seasonal regimes, during the mid Holocene; e) evidence of rain-washing as an important geomorphic agent since the end of MIS 3, at least, until the mid Holocene; f) evidence of mixed grasslands and forests around LGM topographic summits; g) pollinic, isotopic and sedimentologic evidence of climate changes more complex than the "warming and wet vs. cooling and dry" classic binomial model for the humid tropics; h) evidence of secular adaptation of vegetation and geomorphic systems to climatic changes at the Late Pleistocene.

To our knowledge, no similar near-valley head stratigraphic record had been reported before in Brazil, and few in other countries embrace such a wide site-to-site time span. The interpretation stresses the influence of very local controlling factors that seem to respond to regional and global climatic-driven processes. Under similar local environmental conditions, the observed sedimentary pattern may reflect regional trends, affecting southern Brazilian highlands. This pattern suggests that near-valley head slopes and channels had evolved under the influence of local shallow soil-water saturated zones. Stadials would imply drier climate periods, but lower temperatures and lower evaporation rates still would support local saturated zones, improving the development of umbric epipedons, the formation of peat deposits and pulses of overland flow and mass

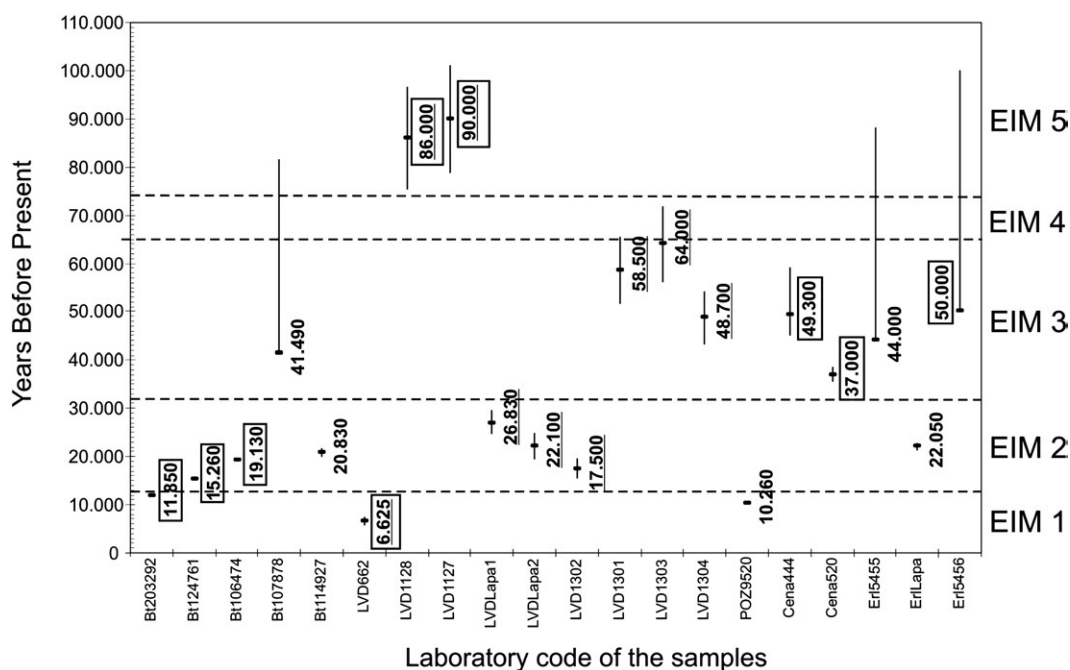


Fig. 17. Independent radiocarbon and luminescence ages reported for the Southern Brazilian States of Paraná, Santa Catarina and Rio Grande do Sul. Luminescence ages are underlined. The ages inside the rectangles refer to study results. Note the distribution of dating with respect to main Late Pleistocene marine isotopic stages (MIS). The figure was compiled after Oliveira et al. (2001), Camargo (2005), Camargo Filho (2005) and Fett (2005).

781 movements on the slopes. During dryer periods, mostly warming but
782 also cooling, rain-wash erosion would be more influential.

783 This recurrent concentration of hydrologic-driven processes
784 through time is perhaps one of the most important influences of
785 valley head areas on the adaptation of drainage net systems to
786 environmental changes (Dietrich and Dunne, 1993). As a result, near-
787 valley head areas deserve further attention in Quaternary studies
788 since, besides their alleged sensitiveness and resilience, these areas
789 also express unambiguous short source-to-sink sedimentary path-
790 ways, generally improving the quality of the stratigraphic record. The
791 Southern Brazilian highlands, under relatively mild climate today,
792 probably constitute a special terrain for preservation and study of
793 near-valley head Quaternary deposits. The verification of a similar
794 record in other countries may represent a clear contribution of
795 geomorphology to the improvement of Quaternary studies.

796 Acknowledgement

797 This research was supported by CNPq (Brazilian National Research
798 Council).

799 References

- 800 Aharon, P., Chappell, J., 1986. Oxygen isotope sea-level changes and the temperature
801 history of a coral reef environment in New Guinea over the last 10⁵ years.
802 *Palaeogeography, Palaeoclimatology, Palaeoecology* 56, 337–352.
803 Bard, E., Rostek, F., Sonzogni, C., 1997. Interhemispheric synchrony of the last
804 deglaciation inferred from alkenone palaeothermometry. *Nature* 385, 707–710.
805 Behling, H., 1993. *Untersuchungen zur spätpleistozänen und holozänen Vegetations-
806 und Klimageschichte der tropischen Küstenwälder und der Araukarienwälder in
807 Santa Catarina (Südbrasilien)*. Dissertationes Botanicae 206, J. Cramer, Berlin,
808 Stuttgart.
809 Behling, H., 1997a. Late Quaternary vegetation, climate and fire history in the *Araucaria*
810 forest and campos region from Serra Campos Gerais (Paraná), S Brazil. *Review of
811 Palaeobotany and Palynology* 97, 109–121.
812 Behling, H., 1997b. Late Quaternary vegetation, climate and fire history from the tropical
813 mountain region of Morro de Itapeva, SE Brazil. *Palaeogeography, Palaeoclimatol-
814 ogy, Palaeoecology* 129 (3–4), 407–422.
815 Benvenuti, M., Carnicelli, S., Belluomini, G., Dainelli, N., Di Grazia, S., Ferrari, G.A., Iasio,
816 M., Sagri, M., Ventra, D., Atnafu, Balemwald, Kebede, Seifu, 2002. The Ziway-Shala
817 lake basin (main Ethiopian rift, Ethiopia): a revision of basin evolution with special
818 reference to the Late Quaternary. *Journal of African Earth Sciences* 35, 247–269.

- Bertran, P., Texier, J.P., 1999. Facies and microfacies of slope deposits. *Catena* 35, 99–121. 819
Bertran, P., Jomelli, V., 2000. Post-glacial colluvium in western Norway: depositional 820
processes, facies and palaeoclimatic record. *Sedimentology* 47, 1053–1068. 821
Bigarella, J.J., Mousinho, M.R., 1965. Considerações a respeito dos terraços fluviais,
822 rampas de colúvio e várzeas. *Boletim Paranaense de Geografia* 16/17, 153–197. 823
Biondi, J.C., Bartoszek, M.K., Vanzela, G.A., 2001. Controles geológicos e geomorfológicos
824 dos depósitos de caulim da bacia de Campo Alegre (SC). *Revista Brasileira de
825 Geociências* 31, 13–20. 826
Blunier, T., Brooks, E.J., 2001. Timing of millennial-scale climate change in Antarctica and
827 Greenland during the Last Glacial period. *Science* 291, 109–112. 828
Blunier, T., Schwander, I., Stocker, T.F., Dallenbach, A., Indermuhle, A., Tschumi, J.,
829 Chappellaz, I., Raynaud, D., Barnola, J.M., 1997. Timing of the Antarctic atmospheric
830 CO₂ increase with respect to the Younger Dryas event. *Geophysical Research Letters*
831 24, 2683–2686. 832
Blunier, T., Chappellaz, I., Schwander, I., Dallenbach, A., Stauffer, B., Stocker, T.F.,
833 Raynaud, D., Jouzel, J., Clausen, H.B., Hammer, C.U., Johnsen, S.J., 1998. Asynchrony of
834 Antarctica and Greenland climate during the last glacial. *Nature* 394, 739–734. 835
Bond, G., Broecker, W., Johnsen, S., McManus, J., Labeyrie, L., Jouzel, J., Bonani, G., 1993.
836 Correlations between climate records from North Atlantic sediments and Green-
837 land ice. *Nature* 365, 143–147. 838
Broecker, W.S., 1995. Cooling the tropics. *Nature* 376, 212–213. 839
Bullock, P., Fedoroff, N., Jongerius, A., Stoops, G., Tursina, T., 1985. *Handbook of soil thin
840 section description*. Waine Research, Albrington. 841
Camargo, G., 2005. O significado paleoambiental de depósitos de encosta e de
842 preenchimento de canal no município de Lapa, no sul do Segundo Planalto
843 Paranaense. Ph.D. Thesis, Geografia - Universidade Federal de Santa Catarina,
844 Florianópolis, Santa Catarina, Brazil. 845
Camargo Filho, M., 2005. O significado paleoambiental de seqüência pedossedimentar
846 em baixa-encosta: o caso dos paleossolo Monjolo, Lapa, PR. Ph.D. Thesis, Geografia -
847 Universidade Federal de Santa Catarina, Florianópolis, Santa Catarina, Brazil. 848
Clark, P.U., Mitrovica, J.X., Milne, G.A., Tamisiea, M.E., 2002. Sea-Level Fingerprinting as a
849 direct test for the source of Global Meltwater Pulse IA. *Science* 295, 2438–2441. 850
Coltrani, L., 1993. Global Quaternary changes in South America. *Global and Planetary*
851 *Change* 7, 11–23. 852
Cortese, G., Abelman, A., 2002. Radiolarian-based paleotemperatures during the last
853 160 kyr at ODP site 1089 (Southern Ocean, Atlantic Sector). *Palaeogeography,
854 Palaeoclimatology, Palaeoecology* 182, 259–286. 855
De Keyser, T.L., 1999. Digital scanning of thin sections and peels. *Journal of Sedimentary*
856 *Research* 69, 962–964. 857
Delvigne, J., 1998. *Atlas of Micromorphology of Mineral Alteration and Weathering*. The
858 *Canadian Mineralogist, Special publication 3*, Mineralogical Association of Canada
859 and ORSTOM Éditions. 860
Dietrich, W.E., Dunne, T., 1993. The channel head. In: Beven, K., Kirkby, M.J. (Eds.),
861 *Channel network hydrology*. John Wiley and Sons, New York, pp. 175–219. 862
Fard, A.M., 2001. Recognition of abrupt climate changes in clastic sedimentary
863 environments: an introduction. *Global and Planetary Change* 28, 9–12. 864
Fernandes, N.F., Dietrich, W.E., 1996. Modeling hillslope evolution under cyclic climatic
865 oscillations: the time required to steady-state. *Anais da Academia Brasileira de
866 Ciências* 68, 157–162. 867

- 868 Ferreira, G.M.S.S., Oliveira, M.A.T., 2006. Aplicação da micromorfologia de solos ao
869 estudo de sedimentos alúvio-colúviais em cabeceiras de vale. *Pesquisas em*
870 *Geociências* 33 (2), 3–18.
- 871 Fett, N. Jr., 2005. Aspectos morfológicos, estratigráficos e sedimentológicos de depósitos
872 quaternários no curso médio do Rio Pardo (município de Candelária, RS). M.Sc.
873 Thesis, Geografia - Universidade Federal de Santa Catarina, Florianópolis, Santa
874 Catarina, Brazil.
- 875 Finkl Jr., C.W., 1984. Chronology of weathered materials and soil age determination in
876 pedostratigraphic sequences. *Chemical Geology* 44 (1–3), 311–335.
- 877 Flemming, B.W., 2000. A revised textural classification of gravel-free muddy sediments
878 on the basis of ternary diagrams. *Continental Shelf Research* 20, 1125–1137.
- 879 Folk, R.L., 1974. The petrology of sedimentary rocks. Hemphill Publishing Co., Austin.
- 880 Grimm, E.C., 1987. Coniss: a Fortran 77 program for stratigraphically constrained cluster
881 analysis by the method of the incremental sum of squares. *Computer and*
882 *Geosciences* 13, 13–35.
- 883 Grimm, A.M., Barros, V.R., Doyle, M.E., 2000. Climate variability in Southern South
884 America associated with El Niño and La Niña events. *Journal of Climate* 13, 35–58.
- 885 Iriondo, M., 1999. Climatic changes in the South American plains: records of a continent-
886 scale oscillation. *Quaternary International* 57/58, 93–112.
- 887 Lima, G.L., 2005. Caracterização pedostratigráfica de depósitos de encosta e de vale,
888 localidade de Cerro do Touro, Campo Alegre, Estado de Santa Catarina. M.Sc. Thesis,
889 Geografia - Universidade Federal de Santa Catarina, Florianópolis, Santa Catarina,
890 Brazil.
- 891 Meis, M.R.M., Machado, M.B., 1978. A morfologia de rampas e terraços do Médio Vale do
892 Rio Doce. *Finisterra* 13, 201–218.
- 893 Meis, M.R.M., Monteiro, A.M.F., 1979. Upper Quaternary "Rampas", Doce River Valley, SE
894 Brazilian Plateau. *Zeitschrift für Geomorphologie* 232, 132–151.
- 895 Meis, M.R.M., Moura, J.R.S., 1984. Upper quaternary sedimentation and hillslope
896 evolution: Southeastern Brazilian plateau. *American Journal of Science* 284, 241–254.
- 897 Melo, M.S., Cuchierato, G., 2004. Quaternary colluvial-eluvial covers of the Eastern
898 Paraná Basin, Southeastern Brazil. *Quaternary International* 114, 45–53.
- 899 Melo, M.S., Coimbra, A.M., Cuchierato, G., 2001. Genesis of Quaternary colluvial-eluvial
900 covers in Southeastern Brazil. *Quaternaire* 12 (3), 179–188.
- 901 Miall, A.D., 1985. Architectural-element analysis: a new method of facies analysis
902 applied to fluvial deposits. *Earth Science Reviews* 22, 261–308.
- 903 Modenesi-Gauttieri, M.C., 2000. Hillslope deposits and the Quaternary evolution of the
904 *Altos Campos* - Serra da Mantiqueira, from Campo do Jordão to the Itatiaia Massif.
905 *Revista Brasileira de Geociências* 30, 504–510.
- 906 Moro, R.S., Bicudo, C.E.M., Melo, M.S., Schmitt, J., 2004. Paleoclimate of the late
907 Pleistocene and Holocene at Lagoa Dourada, Paraná State, southern Brazil.
908 *Quaternary International* 114, 87–99.
- 909 Moura, J.R.S., Mello, C.L., 1991. Classificação aloestratigráfica do Quaternário Superior da
910 região de Bananal (SP/RJ). *Revista Brasileira de Geociências* 21 (3), 236–254.
- 911 Moura, J.R.S., Peixoto, M.N.O., Silva, T.M., 1991. Geometria do relevo e estratigrafia do
912 Quaternário como base à tipologia de cabeceiras de drenagem em anfiteatro -
913 Médio Vale do Rio Paraíba do Sul. *Revista Brasileira de Geociências* 21 (3), 255–265.
- 914 Nemec, W., Kazanci, N., 1999. Quaternary colluvium in west-central Anatolia:
915 sedimentary facies and palaeoclimatic significance. *Sedimentology* 46, 139–170.
- 916 Oliveira, M.A.T., Pereira, K.N., 1998. Identificação de Solos Colúviais em Áreas de
917 Cabeceira de Drenagem: Cerro do Touro, Campo Alegre (SC). *Revista Geosul* 14 (27),
918 476–481.
- 919 Oliveira, M.A.T., Lima, G.L., 2004. Classificação de sedimentos quaternários em
920 cabeceiras de vale através da aplicação do diagrama de Flemming: município de
921 Campo Alegre, Norte de Santa Catarina. *Revista Geociências* 23 (1/2), 67–78.
- Oliveira, M.A.T., Camargo, G., Paisani, J.C., Camargo Filho, M., 2001. Caracterização
922 paleohidrológica de estruturas sedimentares quaternárias através de análises
923 macroscópicas e microscópicas: do registro sedimentar local aos indícios de
924 mudanças globais. *Pesquisas em Geociências* 28, 183–195.
925
- Oliveira, M.A.T., Pessenda, L.C.R., Behling, H., Lima, G.L., Ferreira, G.M.S.S., in press.
926 Registro de mudanças ambientais pleistocênicas e holocênicas em depósitos de
927 cabeceira de vale: Campo Alegre, Planalto Norte catarinense (SC). *Revista Brasileira*
928 *de Geociências* 36 (2).
929
- Pessenda, L.C.R., Gouveia, S.E.M., Aravena, R., Boulet, R., Valencia, E.P.E., 2004. Holocene
930 fire and vegetation changes in southeastern Brazil as deduced from fossil charcoal
931 and soil carbon isotopes. *Quaternary International* 114 (9), 35–43.
932
- Peterson, L.C., Haug, G.H., Hughen, K.A., Röhl, U., 2000. Rapid changes in the hydrologic
933 cycle of the tropical Atlantic during the last glacial. *Science* 290, 1947–1951.
934
- Schaefer, J.M., Denton, G.H., Barrel, D.J.A., Ivy-Ochs, S., Kubik, P.W., Andersen, B.G.,
935 Philips, F.M., Lowell, T.V., Schlüchter, C., 2006. Near-synchronous interhemispheric
936 termination of the last glacial maximum in mid-latitudes. *Science* 312 (5779),
937 1510–1513.
938
- Scholle, P.A., 1979. A color illustrated guide to constituents, textures, cements and
939 porosities of sandstones and associated rocks. American Association of Petroleum
940 Geologists, Memoir 28, Tulsa.
941
- Servant, M., Soubiès, F., Suguio, K., Turcq, B., Fournier, M., 1989. Alluvial fans in
942 Southeastern Brazil as an evidence for early Holocene dry climate period. *943*
International Symposium on Global Changes in South America During the
944 *Quaternary, Special Publication 1. ABEQUA-INQUA, São Paulo, pp. 75–77.*
945
- Shotyk, W., 1992. Organic soils. In: Martini, I.P., Chesworth, W. (Eds.), *Weathering, Soils*
946 *and Paleosoils. Developments in Earth Surface Processes, vol. 2. Elsevier,*
947 *Amsterdam, pp. 203–224.*
948
- Sowers, T.A., Bender, M., 1995. Climate records covering the last glaciation. *Science* 269,
949 210–214.
950
- Stevaux, J.C., Santos, M.L., 1998. Palaeohydrological changes in the Upper Paraná River,
951 Southeastern Brazil as an evidence for early Holocene dry climate period. In: Benito, G., Baker, V.R.,
952 Gregory, K.J. (Eds.), *Palaeohydrology and Environmental Change. John Wiley and*
953 *Sons, Chichester, pp. 273–285.*
954
- Sugden, D.E., Bentley, M.J., Fogwill, C.J., Hulton, N.R.J., McCulloch, R.D., Purves, R.S., 2005.
955 Late-glacial glacier events in southernmost South America: a blend of "northern"
956 and "southern" hemispheric signals? *Geografiska Annaler* 87(A), 273–288.
957
- Thomas, M.F., 2004. Landscape sensitivity to rapid environmental change - a
958 Quaternary perspective with examples from tropical areas. *Catena* 55, 107–124.
959
- Thomas, M.F., Thorp, M.B., 1996. The response of geomorphic systems to climate and
960 hydrological change during the Late Glacial and early Holocene in the humid and
961 sub-humid tropics. In: Branson, J., Thomas, M.F., Nott, J., Price, D.M. (Eds.), *Global*
962 *Continental Changes: the Context of Palaeohydrology, Geological Society Special*
963 *Publication 115. London, pp. 139–154.*
964
- Thomas, M.F., Nott, J., Price, D.M., 2001. Late Quaternary sedimentation in the humid
965 tropics: a review with new data from NE Queensland, Australia. *Geomorphology* 39,
966 53–68.
967
- Turcq, B., Pressinotti, M.N., Martin, L., 1997. Paleohydrology and paleoclimate of the past
968 33,000 years at the Tamanduá river, Central Brazil. *Quaternary Research* 47,
969 284–294.
970
- Wasson, R.J., Claussen, M., 2002. Earth system models: a test using the mid-Holocene in
971 the Southern Hemisphere. *Quaternary Science Reviews* 21, 819–824.
972
- Weaver, A.J., Saenko, O.A., Clark, P.U., Mitrovica, J.X., 2003. Meltwater pulse 1A from
973 Antarctica as a trigger of the Bølling-Allerød warm interval. *Science* 299,
974 1709–1713.
975